A Round-Robin Study of Cellulose Pyrolysis Kinetics by Thermogravimetry

Morten Grønli

SINTEF Energy Research, Thermal Energy and Hydropower, 7034 Trondheim, Norway
Email: morten.g.gronli@ntnu.no

Michael Jerry Antal, Jr.*

Hawaii Natural Energy Institute, University of Hawaii at Manoa, Honolulu, Hawaii 96822,
Email: mantal@hawaii.edu

Gábor Várhegyi

Research Laboratory for Materials and Environmental Chemistry, Chemical Research Center,
Hungarian Academy of Sciences, Email: varhegyi.gabor@t-online.hu or gvarhegyi@gmail.com

Abstract

Eight European laboratories with access to five different thermogravimetric analyzers participated in this round-robin study of Avicel PH-105 cellulose pyrolysis at 5 and 40 °C/min. Agreement between the laboratories on the temperature (T_{peak}) associated with the maximum rate of weight loss at 5 °C/min was good. Less agreement was obtained on the residual char yield. At 40 °C/min, the scatter associated with measurements of T_{peak} and the char yield increased. Good fits to each weight loss curve were obtained by use of a kinetic model based on an irreversible, first order reaction with a high (ca. 244 kJ/mol) apparent activation energy (E). Variations in values of E and the pre-exponential constant (A) are attributed to variations in thermal lag between the various instruments, and at different heating rates. Kinetic parameters are presented which offer a good fit to the 5 °C/min round-robin data, and which prescribe an envelope that contains the data. We recommend that future studies of biomass pyrolysis by thermogravimetry include an analysis of Avicel PH 105 cellulose at 5 °C/min, and a comparison of the resulting weight loss curve with the curves presented herein.

Introduction

Almost 20 years ago Chornet and Roy[1] called attention to gross disagreements in the literature concerning the kinetics of cellulose pyrolysis. At about the same time, Antal et al.[2] reported systematic temperature shifts of 20 - 25°C at all heating rates in a Dupont 951 thermogravimetric analyzer, depending upon whether the sample thermocouple was placed slightly upstream or slightly downstream of a 2 mg

cellulose sample. Since that time, many more papers have appeared in the literature, yet there is still no consensus concerning the kinetics of cellulose pyrolysis.[3] One explanation for the disagreements is the potential role of varied systematic errors in temperature measurement among the various thermobalances used by researchers.[4,5] Systematic errors comparable to those reported by Antal et al.[2] can explain the widely scattered values of the activation energy and pre-exponential constant recorded in the literature.[6]

   To test this hypothesis we organized a round-robin study of cellulose pyrolysis kinetics by thermogravimetry, whose results are recorded in this paper. The organization of this round-robin benefited from the experience gained by one of the authors (MG) in an earlier study[7] that involved three different laboratories. The present round-robin included five widely used thermobalances. All conventional designs for accurate measurement of weight loss and temperature in a heated environment were represented. We deliberately permitted each laboratory to employ its own standard procedures related to gas flows, buoyancy corrections, etc. (see below) in order to obtain a realistic assessment of scatter in the data. Future round-robin studies may wish to strictly define these procedures at the outset. To the best of our knowledge, this is the first round-robin study of the kinetics of cellulose pyrolysis reported in the literature.

Table 1. Characteristics of the instruments used in the round robin study.

	TA Instruments SDT 2960	Perkin Elmer TGS 2/TGA 7	Mettler Toledo TGA/SDTA 851^e	Netzsch STA 409C
Balance sensitivity:	0.1 µg	0.1 µg	0.1 µg	1.25 µg
Sample capacity:	200 mg	130 mg	1000 mg	2000 mg
Thermocouple location:	below and in contact with crucible holder	below sample holder	below and in contact with crucible holder	below and in contact with crucible holder
Calibration:	melting point of different metal standards	curie point of different metal standards	melting point of different metal standards	melting point of different metal standards
Flow rates employed in the study (ml/min):	100 – 500	75 – 140	30	100
Sample holder				
Material:	Platinum	Platinum	Platinum-Rhodium	Platinum-Rhodium
			15.0	6.0
Diameter (mm):	6.0	5.2 – 6	1.5	4.0
Height (mm):	3.0	1.4		

TA Instruments SDT 2960   Perkin Elmer TGS 2   Netzsch STA 409C
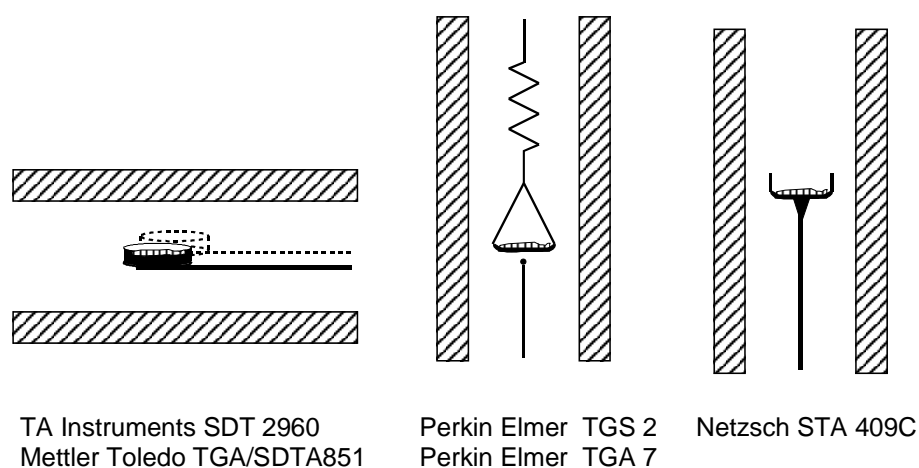Mettler Toledo TGA/SDTA851   Perkin Elmer TGA 7

Figure 1. Schematics of the thermobalances used in this round-robin. (The dashed lines represent the reference sample pan of TA SDT 2960.)

Apparatus and Experimental Procedures

Eight laboratories participated in this round-robin study (see the Acknowledgments section). These laboratories employed the following thermogravimetric analyzers: three *TA Instruments model SDT 2960,* two *Perkin Elmer model TGA7,* a *Perkin Elmer model TGS2,* a *Mettler Toledo model TGA/SDTA 851^e*, and a *Netzsch STA 409C* instrument. Figure 1 displays schematics of these five thermobalances, and Table 1 summarizes the manufacturers' technical specifications of these instruments. Table 1 also lists some details of the experimental conditions and procedures employed by each laboratory. We remark that each participant in this study has had considerable experience with thermogravimetric analysis.

The results we present represent each laboratory's independent analysis of the sample, without knowledge of the results obtained from the other laboratories (except those results that were already available in the archival literature).

Prior to the initiation of the round-robin we selected heating rates of 5 and 40°C/min for study. The lower rate was chosen to minimize systematic errors in temperature measurement due to thermal lag during pyrolysis; whereas the higher rate was employed to evoke some thermal lag. Likewise, we asked our collaborators to use small sample masses ($\leq$ 5 mg) in the experiments to further minimize the influences of heat and mass transfer. The actual sample masses (m_0) employed by the different laboratories at the two heating rates are displayed in Tables 2 and 3. Note that many of the participants reduced the sample mass that they employed at the higher heating rate (see Table 3) to decrease the impact of heat and mass transfer limitations on the experimental measurements. Also, the Hungarian Academy of Sciences (HAS) executed additional experiments with sample masses in the range 0.1 to 1.0 mg to offer insight into the effects of sample size on results at the higher heating rate. All the participants (except the HAS) used flowing nitrogen as the inert purge gas. The HAS used high purity argon to maintain consistency with its earlier work.

All analyses reported in this paper employed Avicel PH-105 microcrystalline cellulose samples taken from the same can, that was obtained from FMC Corporation in 1985. This can was first opened in 1996, and (except for occasional withdrawals of sample), has remained sealed and stored at room temperature in Honolulu during the past two years. In an earlier paper[3] we compared studies of samples taken from this can to samples of Avicel PH-105 cellulose taken from other cans stored in Honolulu and opened in 1990 and 1986. Over the ten year period the reproducibility of thermogravimetric analyses of samples taken from these three different lots of Avicel cellulose was good.[3] Thus, a considerable amount of evidence exists to support the hypothesis that the thermal properties of Avicel cellulose remain unchanged during storage in air at room temperature over a period of years. Also, Avicel cellulose is available in bulk and is not expensive. For these reasons, we believe it to be a suitable standard sample for use within the biomass community.
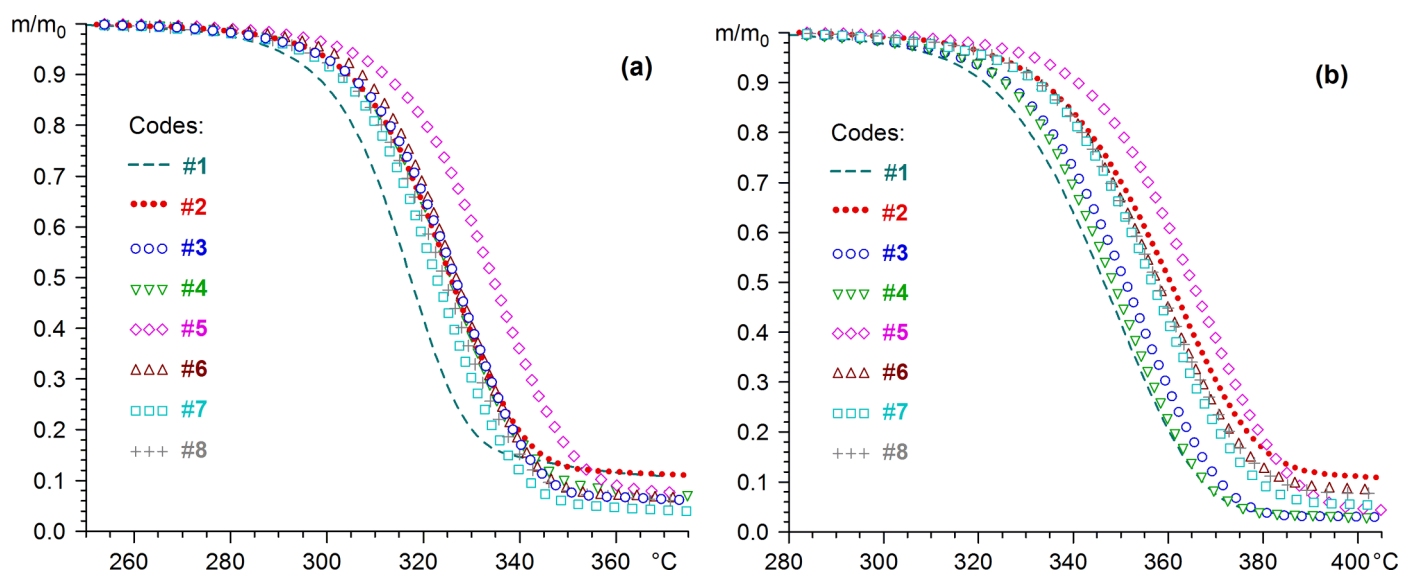

Figure 2. TG curves recorded by the round-robin participants at 5 °C/min (a) and 40 °C/min (b).

Kinetic Analysis

The kinetic analyses presented in this paper are based on the first-order rate equation:

$$\frac{d\alpha}{dt} = k\,(1 - \alpha) \tag{1}$$

where $\alpha = 1-(m(t) - m_f)/(m_0 - m_f)$, $k = A \exp(-E/RT)$, $m(t)$ is the time dependent sample mass, m_0 is the initial, dry sample mass, m_f is the final sample mass, A is the pre-exponential constant, E is the apparent activation energy, R is the gas constant, and T is the sample temperature. Earlier work has shown that a first-order model offers a good fit to weight loss curves obtained at a single heating rate,[3] and that differences in kinetic parameters obtained at different heating rates can be attributed to thermal lag.[3,4] These matters will be examined in greater detail below.

In addition to the parameters A and E, equation (1) depends upon the measured values of the initial sample mass (m_0) and the mass of the char residual (m_f). In spite of our efforts to standardize the procedures employed by the round-robin participants, minor ambiguities appeared in the determination of m_0 and m_f. These ambiguities resulted from the following instrumental and procedural subtleties. (i) The slope of the baseline (empty pan) thermogravimetric (TG) curve of each participant differed slightly due to differing sensitivities of each instrument to the buoyancy effect.   (ii) Some of the participants automatically subtracted the TG curve of an empty pan experiment from their Avicel data to correct for baseline drift. (iii) Some of the participants employed an isothermal drying period prior to the onset of heating at the prescribed rate. To minimize the effects of these factors on the kinetic analysis, we defined the mass of the dry cellulose sample (m_0) to be the measured TG value at a temperature safely above that needed to ensure dryness, but before the onset of pyrolysis (see below). We also employed m_f/m_0 as a parameter in the non-linear least squares kinetic analysis of the data.   This approach incorporates ambiguities in the determination of m_f and m_0 into the parameter m_f/m_0, and frees the parameters E and A from the impact of these ambiguities. In the Tables containing the results we list the last observed value of m/m_0 in the interval of evaluation, m_{last}/m_0, as well as the m_f/m_0 parameter determined by the kinetic evaluation.

Our kinetic analysis of the participants' data used non-linear least squares (NLS) algorithms which identified parameters (A, E, and m_f/m_0) that minimized values of the objective functions S_{TG} given below.

$$S_{TG} = \sum_{j=1}^{N} \left((m)_j^{exp} - (m)_j^{calc} \right)^2 \tag{2}$$

In equation 2 $(m)^{exp}$ is the experimentally observed TG mass measurement, and $(m)^{calc}$ is the calculated mass value obtained by numerical solution of the first-order rate equation with the given set of parameters. Subscript j denotes discrete values of m, and N is the number of data points used in the least squares evaluation. To account for different systematic errors in sample temperature measurement manifested by each of the different instruments (see below), values of the objective function S_{TG} were evaluated within an interval that was defined relative to the value of the differential thermogravimetric (DTG) peak temperature (T_{peak}). The starting point of the interval was given by the time at which the measured sample temperature reached T_{peak} - 80°C; whereas the ending point of the interval was given by the time at which the temperature reached T_{peak} + 50°C. Likewise, the initial dry sample mass (m_0) was determined to be the TG value at T_{peak} - 80 °C. The fit of the calculated TG curve to the experimental curve at the optimal set of parameters is given by:

$$dev(\%) = 100 \, (S_{TG}/N)^{0.5} / m_0 \tag{3}$$

Two independently developed programs were used for the NLS analysis. The Norwegian University of Science and Technology (NTNU) program was written in Matlab 4.0 operating under Windows NT.[7] The HAS program was written in Fortran 90 operating under Windows 95.[8,9] This program runs as a

"console application" and passes the results to another Windows application program written in C++ for graphic display. Although the algorithms employed by the two laboratories were different, the values of the best-fit parameters identified by each program were essentially identical.
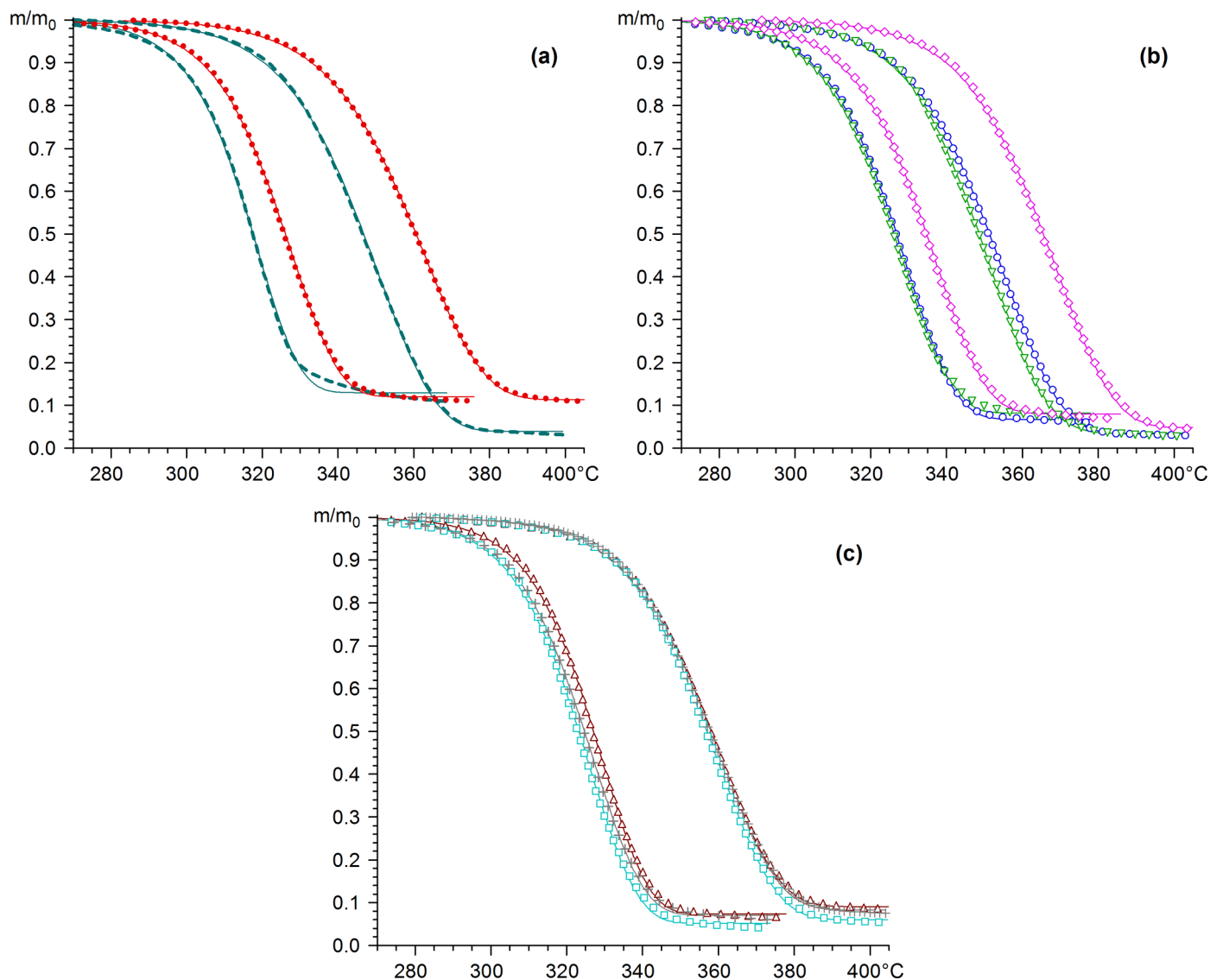

Figure 3. Kinetic evaluations of the TG curves. Kinetic parameters used to create the best-fitting curves (——) for each instrument are listed in Table 2 (5 °C/min) and Table 3 (40 °C/min). (a) Instruments #1 and 2. (b) Instruments #3, 4, and 5. (c) Instruments #6, 7, and 8.

Table 2. Kinetic evaluation of Avicel cellulose TG curves at a nominal heating rate of 5°C/min. (See Figure 3.)

Instrument number and graphic symbol	m_0 (mg)	dT/dt (°C/min)	T_{peak} (°C)	$100\ m_{last}/m_0$ (% of m_0)	E (kJ/mol)	$\log A$ ($\log s^{-1}$)	$100\ m_f/m_0$ (% of m_0)	Fit (%)
#1 (-)	4.7	5.0	319[a]	10.9	263	21.1	13.0	0.9
#2 (•)	5.1	5.0	326[a]	10.9	242	18.9	12.0	0.5
#3 (o)	2.0	4.8	328[b]	6.0	236	18.3	6.7	0.4
#4 (∇)	5.1	5.0	327[a]	6.9	241	18.8	8.2	0.6
#5 (◊)	4.8	5.1	336[a]	6.8	234	17.8	8.0	0.5
#6 (Δ)	4.2	5.0	328[b]	6.4	257	20.1	7.4	0.6
#7 (∇)	2.2	5.0	324[b]	4.0	241	18.8	5.2	0.6
#8 (+)	4.7	5.0	326[b]	5.9	238	18.5	7.0	0.6
Means	4.1	5.0	327	7.2	244	19.0	8.4	0.6
Deviations	1.3	0.1	5	2.4	10	1.1	2.7	0.2

[a] The DTG curve was calculated by the authors.
[b] The DTG values were provided by the participants.

Table 3. Kinetic evaluation of Avicel cellulose TG curves at a nominal heating rate of 40°C/min. (See Figure 3.)

Instrument number and graphic symbol	m_0 (mg)	dT/dt (°C/min)	T_{peak} (°C)	$100\ m_{last}/m_0$ (% of m_0)	E (kJ/mol)	$\log A$ ($\log s^{-1}$)	$100\ m_f/m_0$ (% of m_0)	Fit (%)
#1 (-)	2.7	40.0	350[a]	3.1	211	16.3	3.9	0.4
#2 (•)	5.0	43.0	363[a]	10.5	212	16.1	11.3	0.3
#3 (o)	0.9	38.5	354[b]	3.0	217	16.6	3.3	0.3
#4 (∇)	1.2	41.7	354[a]	2.9	230	17.9	3.4	0.4
#5 (◊)	1.1	41.8	367[a]	3.8	232	17.5	4.8	0.6
#6 (Δ)	1.0	39.8	359[b]	8.3	222	16.9	9.1	0.5
#7 (∇)	1.7	39.5	358[b]	5.2	227	17.4	6.0	0.4
#8 (+)	1.2	39.0	359[b]	7.4	223	17.0	8.3	0.6
Means	1.8	40.4	358	5.5	222	17.0	6.3	0.4
Deviations	1.4	1.6	5	2.9	8	0.6	3.0	0.1

[a] The DTG curve was calculated by the authors.
[b] The DTG values were provided by the participants.

Results and Discussion

Figures 2a and 2b display results obtained by the round-robin participants at 5 and 40 °C/min (respectively). As expected, the 5 °C/min curves enjoy generally good agreement: values of T_{peak} (see Table 2) fall within a range of 17 °C. Instrument #5 recorded weight loss at the highest temperatures, and Instrument #1 at the lowest temperatures. Differences in temperature measurement can result from different temperature correction algorithms employed by the operators. The operator of Instrument #5

mentioned to us that the thermocouple employed in his instrument had not been re-calibrated for several months prior to the Avicel experiment. Similarly, Instruments #1 and 2 recorded the highest value of the char residue (m_{last}/m_0), and Instrument #7 the lowest char residue. These differences can result from small errors in the specification of the initial (dry) sample mass, or baseline drift during heating. Note that the values of m_{last}/m_0 (see Table 2) span a range of 4.0 to 10.9%. Obviously, the measurement of the very small Avicel char residue by thermogravimetry lacks precision.

The 40 °C/min curves evidence more scatter. Nevertheless, Instrument #5 continued to record weight loss at the highest temperatures, and Instrument #1 at the lowest temperatures. Likewise, Instrument #2 continued to report the largest value of the char residue; whereas several different instruments concurred on the lowest value (see Table 3). Note that the values of T_{peak} at 40 °C/min span a range of 17 °C, which is identical to the scattering of values at 5 °C/min. These observations suggest that the differences in sample temperature measurement are largely due to different systematic errors in the calibration of the sample thermocouples used by the different instruments. Also, the scatter in the measured values of the char residue remained large: values of m_{last}/m_0 range from 2.9 to 10.5%.

Tables 2 and 3 also display the results of a first order kinetic analysis of the individual weight loss curves at 5 and 40 °C/min (respectively). Fits of the kinetic model (with parameters listed in Tables 2 and 3) to the experimental data are displayed in Figures 3a – 3c. In all cases, the fit of the first order model to an individual weight loss curve is nearly perfect. Values of the apparent activation energy associated with the 5 °C/min data range from 234 to 263 kJ/mol, and values of log (A/s^{-1}) lie between 17.8 and 21.1. (We employ the notation A/s^{-1} to indicate the value of A divided by its unit; hence A/s^{-1} is a unitless number.) At 40 °C/min the values of E range from 211 to 232 kJ/mol, and values of log (A/s^{-1}) lie between 16.1 and 17.9. Although the range of kinetic parameters at each heating rate may appear to be large, in fact it represents only a small difference in experimental data. To illustrate this fact, we used the mean values, and the highest and lowest values of the kinetic parameters taken from the central six curves in Figure 2a to generate simulated weight loss curves and their derivatives at 5 °C/min (see Figure 4). Obviously, differences between the three calculated curves displayed in Figure 4 are small relative to actual differences in the experimental curves displayed in Figure 2a. From this it is evident that the locations and shapes of the experimental weight loss curves at a given heating rate are not overly sensitive to reasonable changes in the values of E, log A, and m_f/m_0.
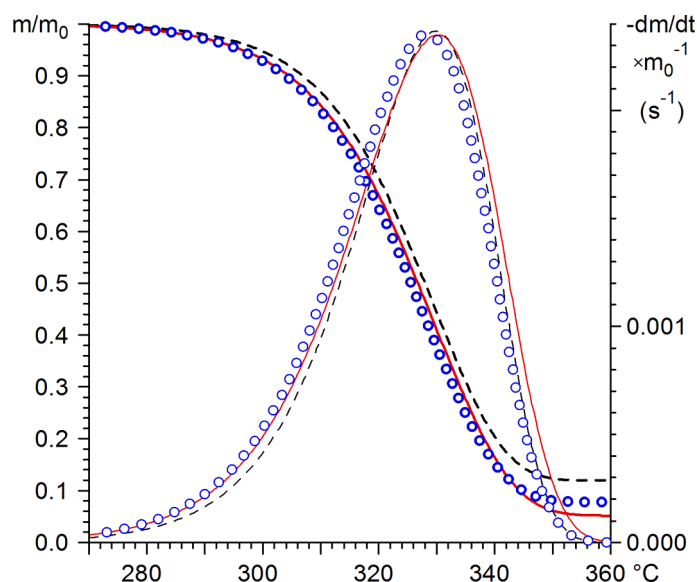
Figure 4. Sensitivity of simulated weight loss at 5 °C/min to values of the kinetic parameters. We display $m^{calc}(t)$ and $m_0^{-1}(-dm^{calc}/dt)$ using the largest parameters (- - - ; E = 256.79, log (A / s^{-1}) = 20.102, m_f/m_0 = 0.1196), the smallest parameters (—— ; E = 236.09, log (A / s^{-1}) = 18.262, m_f/m_0 = 0.0517), and the mean values of the parameters ($\circ\circ\circ$; E = 242.52, log (A / s^{-1}) = 18.892, m_f/m_0 = 0.0775) from kinetic analyses of the data provided by six of the round-robin participants (see text).

The decrease in the values of both E and log A at higher heating rates (compare values in Table 3 to those in Table 2) is a familiar manifestation of the compensation effect. Both this decrease, and the related compensation effect, can result from increased thermal lag at higher heating rates.[6] Systematic errors in temperature measurement, which result from thermal lag, can be reduced by decreasing the size of the sample. Figure 5 illustrates this approach. As the sample size is reduced from 0.95 to 0.11 mg, the thermal lag decreases by 8 °C. Note that this 8 °C decrease represents half of the range of values of T_{peak} determined by the various instruments at 40 °C/min. Table 4 displays kinetic analyses of the curves in Figure 5. Note how the decrease in thermal lag increases the values of E and log A.
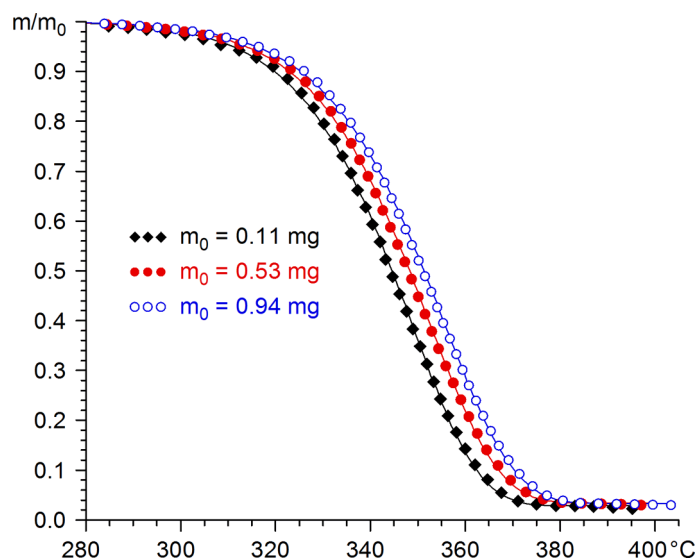
Figure 5. Effect of sample mass on thermal lag inherent in the TG curves measured by Instrument #3 at 40 °C/min.

Table 4. Effect on the sample mass on the kinetic evaluation at a nominal heating rate of 40°C/min as measured by Instrument #3. (See Figure 5).

m_0 (mg)	dT/dt (°C/min)	T_{peak} (°C)	100 m_{last}/m_0 (% of m_0)	E (kJ/mol)	log A (log s^{-1})	100 m_f/m_0 (% of m_0)	Fit (%)
0.11	38.4	346	2.2	224	17.5	2.8	0.4
0.53	38.3	350	2.9	221	17.1	3.4	0.4
0.94	38.5	354	3.0	217	16.7	3.3	0.3
Means:	38.4	350	2.7	220	17.1	3.2	0.4

Our readers may wonder if the temperature shifts displayed in Figure 5 (and elsewhere in this paper) could result from mass transport limitations.[10] It is well known that mass transport limitations can strongly affect the char yield. It is also possible that differences in the gas flow rates, and the exposure of the sample to the gas flow, might explain some of the observed differences between the different instruments employed in this study. Nevertheless, we remark that an increase in resistance to mass transfer lowers the value of T_{peak} for cellulose pyrolysis at a given heating rate.[11-13] But in Figure 5 the values of T_{peak} increase as the sample size (i.e. the resistance to mass transfer) increases. Consequently, we doubt that the temperature shifts displayed in Figure 5 are a result of mass transfer resistances.

One approach to representing the effects of thermal lag on pyrolysis kinetics is to incorporate the uncertainty in the temperature measurement into an uncertainty in the value of log A. As discussed in earlier papers,[3,4,9] this approach has merit because small changes in the value of log A (at constant E) result in temperature shifts of the weight loss curve without significant changes in the actual shape of the curve. Thus the uncertainty in the temperature measurement is represented as an uncertainty in the value of log A. Following this procedure, we fixed the value of the parameter E at the mean value (i.e. 244 kJ/mol) listed in Table 2, and calculated new values of the parameters log A and m_f/m_0 to give a best fit to

each individual weight loss curve (see Table 5). As shown in Figure 6a, the curve which results from the mean values of log A and m_f/m_0 listed in Table 5 offers a good fit to all the weight loss curves at 5 °C/min. Furthermore, we can construct an envelope for all the experimental curves displayed in Figure 2a by use of the largest and smallest values of log A and m_f/m_0 listed in Table 5, and the fixed value E = 244 kJ/mol. This envelope is also displayed in Figure 6a. Note that this envelope nicely incorporates the results of all the participants in this study. Our readers may wonder how the shape and placement of the three calculated weight loss curves change when the heating rate is increased from 5 to 40 °C/min. Figure 6b displays these three curves (which are based on the 5 °C/min parameters), as well as the round-robin experimental data at 40 °C/min, and a similar, first order fit to the high heating rate data. Considering the spread in the round-robin data, the low heating rate kinetic parameters offer a reasonable fit to the higher heating rate data. For example, the curve (open circles) derived from the mean values of the 5 °C/min data in Table 5 is shifted to lower temperatures by only 4 °C from the curve (closed circles) that represents a good fit to the 40 °C/min data. Likewise, the high temperature envelope curve is only about 4 °C lower than the highest temperature experimental data. We believe that thermal lag is responsible for the small differences (ca. 4 °C) that separate the 40 °C/min experimental curves from the calculated curves obtained by use of the 5 °C/min kinetic parameters.

Table 5. Kinetic evaluation of Avicel cellulose TG curves at a nominal heating rate of 5°C/min using the mean value of the apparent activation energy given in Table 2 as a fixed parameter.[a]

Instrument number	E^a (kJ/mol)	log A (log s^{-1})	100 m_f/m_0 (% of m_0)	Fit (%)
#1	244	19.4	12.6	1.1
#2	244	19.0	12.0	0.5
#3	244	19.0	6.9	0.5
#4	244	19.0	8.3	0.6
#5	244	18.7	8.3	0.7
#6	244	19.0	7.1	0.8
#7	244	19.1	5.3	0.6
#8	244	19.1	7.2	0.6
Means	–	19.0	8.5	0.7
Deviations	–	0.2	2.6	0.2

[a] The tables show only the significant digits of the parameters. In the actual calculations the values were not rounded to three digits. Exact values of the parameters are listed in Table 6.

Table 6. List of the mean parameter values with five-digit precision, as they were used in the calculations.

| Description	E (kJ/mol)	log A (log s^{-1})	100 m$_f$/m$_0$ (% of m$_0$)
Means of the parameters in Table 2. (Kinetic evaluation of the 5°C/min experiments.)	243.95	19.027	8.431
Means of the parameters in Table 2 without the experiments with the highest and lowest T$_{peak}$. (See curve ∘∘∘ in Figure 4.)	242.52	18.892	7.747
Means of the parameters in Table 5. (Kinetic evaluation with a fixed E value. See curve ∘∘∘ in Figure 6.)	243.95	19.023	8.451
Highest log A and lowest m$_f$/m$_0$ in Table 5. (See curves ∇∇∇ in Figures 6a and 6b.)	243.95	19.360	5.250
Lowest log A and highest m$_f$/m$_0$ in Table 5. (See curves △△△ in Figures 6a and 6b.)	243.95	18.710	12.570
Means of the parameters in Table 3. (Kinetic evaluation of the 40°C/min experiments. See curve ••• in Figure 6b.)	221.63	16.964	6.261
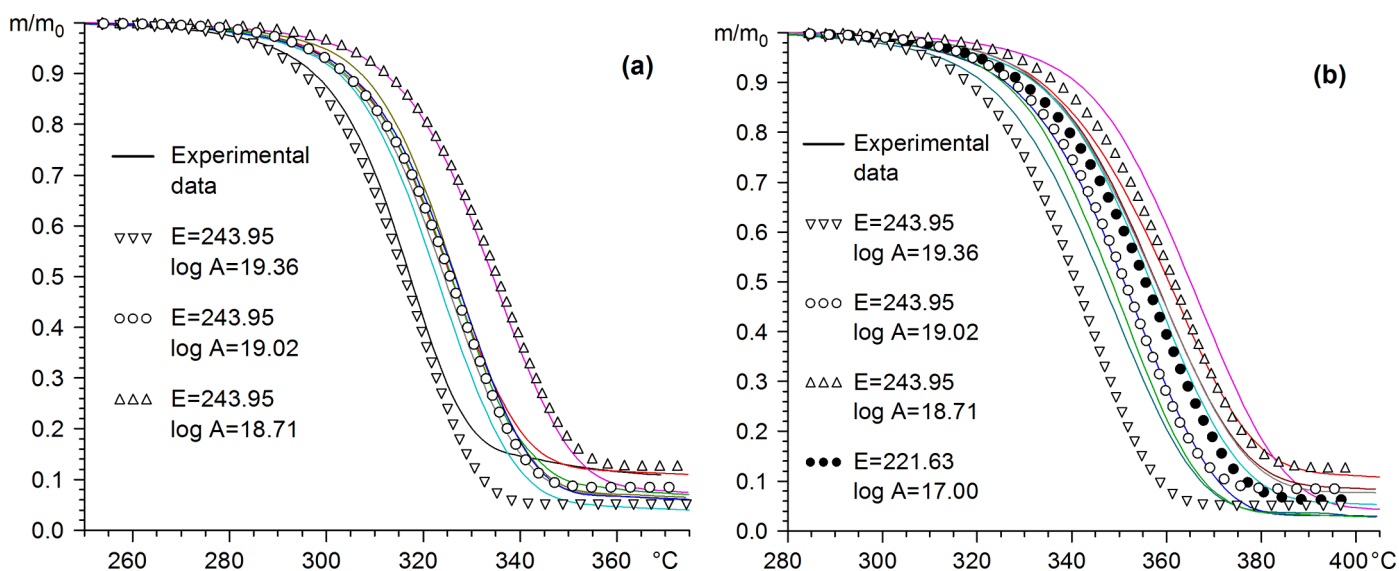
Figure 6. Accord of the first order rate law ∘∘∘ (E = 243.95 kJ/mol, log (A / s^{-1}) = 19.023, and m$_f$/m$_0$ = 0.0845; which are exact values of the means listed in Table 5, with the round-robin results (——) at 5 °C/min (a) and 40 °C/min (b). Kinetic parameters for the two curves △△△ (E = 243.95 kJ/mol, log (A / s^{-1}) = 18.710, and m$_f$/m$_0$ = 0.1257) and ∇∇∇ (E = 243.95 kJ/mol, log (A / s^{-1}) = 19.360, and m$_f$/m$_0$ = 0.0525), which prescribe an envelope for the round-robin results, are the maximum and minimum values of the parameters listed in Table 5. The curve ••• (E = 221.63 kJ/mol, log (A / s^{-1}) = 16.966, and m$_f$/m$_0$ = 0.0626; which are exact values of the means listed in Table 3) in panel (b) represents a good fit to all the round-robin data at 40 °C/min.

Conclusions

1. Good agreement was obtained between all the participants of this round-robin at a low heating rate (5 °C/min). For a fixed value of weight loss, the scatter in the temperature measurement was about 17 °C. Measured values of the char yield lay between 4.0 and 10.9%.

2. All the low heating rate data can be well fit by an irreversible, single step, first order rate equation with a high activation energy (244 kJ/mol). Uncertainty in the temperature measurement can be well represented by a statement of the uncertainty in the value of log A (i.e. log A = 19.0 ± 0.2). Likewise, uncertainty in the residual char measurement can be well represented by a statement of the uncertainty in the value of m_f/m_0.

3. At a higher heating rate (40 °C/min) the agreement was somewhat less good. Scatter in the temperature measurements remained at 17 °C; while the range (2.9 to 10.5%) of values of the char yield increased.

4. Kinetic analyses of the 40 °C/min data resulted in values of E and log A that were somewhat lower than those obtained at 5 °C/min. This decrease in E and log A was attributed to the increased impact of thermal lag on the experimental temperature measurement at the higher heating rate.

5. A decrease in the sample size from 0.95 to 0.11 mg decreased the systematic error due to thermal lag, and increased the values of E and log A. This result is consistent with the hypothesis that thermal lag is largely responsible for the decrease in values of E and log A at higher heating rates.

6. Avicel PH 105 microcrystalline cellulose is stable during storage in air at room temperature over a period of years, and it is widely available in bulk at a low price. We recommend its adoption as a standard for use by scientists concerned with the pyrolysis of organic materials.

7. Mean values of the kinetic parameters listed in Table 5 can be used with the rate law given by Equation 1 to create a curve (see Figure 6a) which represents a good fit to all the experimental data obtained in this round-robin at 5 °C/min. Similarly, the high and low values of log A and m_f/m_0 given in Table 5, together with the fixed value E = 244 kJ/mol, can be used to create curves which prescribe an envelope (see Figure 6a) that contains all the weight loss curves displayed in Figure 2. The exact kinetic parameters used to create these three curves are listed in Table 6. We recommend that future studies of biomass pyrolysis by thermogravimetry include an analysis of Avicel PH 105 cellulose at 5 °C/min, and a comparison of the resulting weight loss curve with the good fit curve, and the envelope of curves discussed above.

8. One reviewer commented: "If a study of this care, with such capable authors, reveals such a significant effect of TGA apparatus, it may be that readers will shy away from TGA as a tool for kinetics analysis, with or without Avicel PH 105 cellulose. I wonder if the authors could comment on this." In our experience, the scatter in experimental data displayed in this paper well represents the

current state-of-the-art. Careful work reported by esteemed colleagues in the prior literature no doubt incurred similar (if not worse) instrumental errors. Modern thermobalance data are beguilingly simple to generate, but not necessarily accurate. Significant uncertainties are present in data obtained from the best state-of-the-art instruments. Unfortunately, we are not aware of any other experimental techniques which offer more reliable data. We are inclined to acknowledge the fact that biomass pyrolysis kinetics are inherently difficult to study by any technique, and these difficulties contribute significant uncertainties to our understanding of the phenomena. In light of this fact, we recommend that all researchers heed the impact of systematic errors on their interpretation of thermobalance data.

Acknowledgement

Nomenclature

α reacted mole fraction

A   preexponential factor (s^{-1})

DTG m_0^{-1} ($-dm^{exp}/dt$) (s^{-1})

E   apparent activation energy (kJ/mol)

fit   deviation between $m^{calc}(t)$ and $m^{exp}(t)$

$m^{calc}(t)$ sample mass calculated from the kinetic equation (mg)

$m^{exp}(t)$ experimental sample mass (mg)

m_0 dry sample mass before the start of cellulose decomposition (defined as m^{exp} at 80°C below T_{peak})

m_f the char yield obtained from the least squares kinetic evaluation

m_{last} the last observed value of m in the interval of evaluation (i.e. m^{exp} at 50°C above T_{peak})

R   gas constant $(kJ\ mol^{-1}\ K^{-1})$

S_{TG} objective function of the least squares evaluation

t   time (s)

T   temperature (°C or K)

T_{peak} DTG peak temperature (°C)

Literature Cited

(1) Chornet, E.; Roy, C. Compensation Effect in the Thermal Decomposition of Cellulosic Materials. *Thermochim. Acta* **1980**, *35*, 389-393.

(2) Antal, M.J.; Friedman, H.L.; Rogers, F.E. Kinetics of Celulose Pyrolysis in Nitrogen and Steam. *Combust. Sci. Technol.* **1980**, *21*, 141-152.

(3) Antal, M.J.; Varhegyi, G.; Jakab, E. Cellulose Pyrolysis Kinetics: Revisited. *Ind. Eng. Chem. Res.* **1998**, *37*, 1267-1275.

(4) Antal, M.J.; Varhegyi, G. Impact of Systematic Errors on the Determination of Cellulose Pyrolysis Kinetics. *Energy Fuels* **1997**, *11*, 1309-1310.

(5) Lanzetta, M.; Di Blasi, C.; Buonanno, F. An Experimental Investigation of Heat Transfer Limitations in the Flash Pyrolysis of Cellulose. *Ind. Eng. Chem. Res.* **1997**, *36*, 542-552.

(6) Narayan, R.; Antal, M.J. Thermal Lag, Fusion, and the Compensation Effect during Biomass Pyrolysis. *Ind. Eng. Chem. Res.* **1996**, *35*, 1711-1721.

(7) Grønli, M.: A Theoretical and Experimental Study of the Thermal Degradation of Biomass. *Ph.D-Thesis, Norwegian University of Science and Technology, Department of Thermal Energy and Hydropower*, **1996**.

(8) Várhegyi, G.; Jakab, E.; Antal, M. J., Jr. Is the Broido - Shafizadeh Model for Cellulose Pyrolysis True? *Energy Fuels* **1994**, *8*, 1345-1352

(9) Várhegyi, G.; Szabó, P.; Jakab, E; Till, F.; Richard, J-R.: Mathematical modeling of char reactivity in Ar-O_2 and CO_2-O_2 mixtures. *Energy Fuels,* **1996,** 10, 1208-1214.

(10) Suuberg, E.M.; Milosavljevic, I.; Oja, V. *26th Symposium (Int.) on Combustion;* The Combustion Institute: Pittsburgh, 1996: pp. 1515-1521.

(11) Várhegyi, G.; Antal, M.J.; Szekely, T.; Till, F.; Jakab, E. Simultaneous Thermogravimetric-Mass Spectrometric Studies of the Thermal Decomposition of Biopolymers. *Energy Fuels,* **1988**, *2*, 267-272.

(12) Mok, W.S.L.; Antal, M.J.; Szabo, P.; Várhegyi, G; Zelei, B. Formation of Charcoal from Biomass in a Sealed Reactor. *Ind. Eng. Chem. Res.* **1992**, 31, 1162-1166.

(13) Várhegyi, G.; Szabo, P.; Mok, W.S.L.; Antal, M.J. Kinetics of the Thermal Decomposition of Cellulose in Sealed Vessels at Elevated Pressures. *J. Anal. Appl. Pyrol.* **1993**, 26, 159-174.